



JOURNAL OF EMERGING TECHNOLOGIES AND INNOVATIVE RESEARCH (JETIR)

An International Scholarly Open Access, Peer-reviewed, Refereed Journal

LUNG CANCER CLASSIFICATION AND IDENTIFICATION USING AN IMPROVED CONVOLUTIONAL NEURAL NETWORK ON COMPUTED TOMOGRAPHY

Raghuel Ganta¹, Dr. B. Leela Kumari²

Department of Electronics and Communication,

University College of Engineering,

Jawaharlal Nehru technological University Kakinada Andhra Pradesh, India

raghueljacks@gmail.com¹, leela8821@yahoo.com²

ABSTRACT

Lung cancer is the most serious illness, with a higher number of deaths in both men and women, making detection difficult. Identification and categorization of lung cancer tumours at an early stage can save the lives of a greater number of patients through correct diagnosis and therapy, lowering the mortality rate and increasing the survival rate. Machine learning technology opens the door to forecast, detect, and categorise this illness, but deep learning under machine learning provides a wide range of options for analysing and evaluating tumour characteristics from CT scans. The approach recommended in this work provides a precise and unambiguous classification for the VGG-16 model and its improved model, which has more hidden layers. The system was trained using the LIDC CT imaging dataset, and the findings reveal that the Improved VGG-16 model and the VGG-16 model both had extremely low false positive rates of 0.0576 and 0.13 and high classification accuracy of 97% and 86%, respectively.

Keywords: Lung Cancer, Computed Tomography, Machine Learning, Deep Networks.

I. INTRODUCTION

Lung cancer is one of the leading causes of mortality, with many fatalities occurring each year in both men and women as a result of this dreadful disease. As a result, a proper technique for detecting and identifying this illness in its early stages should be implemented in order to preserve the lives of a huge number of people suffering from lung cancer. Many patients' survival rates can be improved if it is diagnosed and identified in the early stages. Later on, after illness identification, correct diagnosis can lower patient mortality. So, in order to provide an appropriate and quick result, employing modern machine learning techniques in the medical image processing area by increasing the amount of duplication for the methods used will improve classification accuracy [3]. As a result, accurate early diagnosis and identification will undoubtedly enhance the degree of survival and can reduce the death rate. Medical imaging technology has advanced, and the medical pictures used in most previous research included computed tomography (CT), magnetic resonance, and mammography images. Using appropriate tools, the specialist doctor in this sector analyses and identifies the various degrees of lung cancer [1]. Chemical treatment, targeted therapy, and radiation are among the laboratory and clinical methods used to eliminate or inhibit malignant cell duplications. All of the techniques used to discover and detect cancer disorders are time-consuming, expensive, and uncomfortable for patients [8]. To address all of these issues, appropriate machine learning approaches for analysing these medical pictures, which included CT scan images, were applied. CT scan pictures are chosen above other images because they are less noisy than MRI and X-Ray reports. When compared to radiologists, the procedure of tumour classification and identification has become more accurate and faster with small mistakes throughout the years. In lung cancer, a tumour forms in the lung that causes discomfort or renders the human body useless. As a result, early tumour identification as benign (non-cancerous) or malignant (cancerous) and tumour diagnosis is critical to saving patients from this terrible illness [7]. Improved VGG-16 convolutional neural networks employ a deep learning approach to recognise significant objects in photos. Precise training on vast datasets will improve the network's classification accuracy. In comparison to other image processing techniques, deep learning approaches need the fewest

pre-processing steps. The factors utilised to develop and improve classification accuracy in the VGG-16 include filter size, the number of hidden layers, and extracted features. As network layers go deeper, a high detection level with a high level of feature abstraction may be attained. The deeper the network, the longer the calculation time since there are more Convolutional operations. The assignment is structured as follows: The related work is highlighted in part I, the proposed architecture is described in section II, the findings and comments are described in section III, and the conclusion is summarised in section IV.

II. LITRATURE SERVEY

The Convolutional neural network was utilised for classification using 1006 pictures from the LIDC dataset, yielding 94% accuracy with 90% training and 10% testing images [1]. The author [2] proposes identifying lung nodules using computed tomography scans, which provides sensitivity findings of 90%, increasing patient survival rate. Methods such as the Wiener filter and picture slicing are used to recover the region of interest. To detect lung cancer in its early stages, a 3mm nodule is taken. The author [3] suggested a method for classifying lung nodules using computed tomography images, in which lung segmentation is performed using thresholding and region growth techniques, and image characteristics are retrieved. The retrieved characteristics were sent into the KNN, which subsequently classified the photos. The author offers a Convolutional neural network classifier with an accuracy of roughly 84.6% for recognising lung nodules [4]. In addition, 82.5% sensitivity and 86.7% specificity were attained. It is mentioned that when the dataset amount grows, the degree of illness treatment will rise. The author suggests a model [5] that is used to identify malignant parts of the lung by using deep learning neural network methods; the model has a classification accuracy of around 90% but is unable to determine the kind and category of cancer sickness. The author [6] created a model that diagnoses benign and malignant pictures using support vector machine from computed tomography images and has an accuracy of 83.11%. A model that recognises lung cancer nodules from CT images was described [7], which employs an SVM classifier to enhance efficiency and minimise error rate. The author [8] provided a technique that identifies lung cancer nodules based on their size, which ranges from 3mm to 10mm in the LIDC dataset. The

system employs machine learning algorithms such as K-Nearest Neighbour and Random Forest, and it achieves a classification accuracy of 82%. To categorise cancerous and benign pictures, a Deep Convolutional Neural Network is trained using CT scans from the LIDC dataset. By extracting picture characteristics, the network achieves a sensitivity of 78.9% utilising back propagation methods. The author [9] provided a classification model based on principal component analysis utilising CT images that achieves a 90% accuracy by employing the principal component analysis approach. The model's initial stage is lung organ segmentation, followed by lung nodule segmentation and categorization of benign and malignant pictures. The technique detects disease malignancy in the early stages [10] by going through the illness's stages. The initial stage in the detection phase is pre-processing and segmentation, which enhances classification accuracy by using support vector machine and fuzzy logic classifiers. The classifier recognises and classifies photos as benign or malignant tumours based on the degree intensities of the images. Convolutional neural networks [11] were utilised to separate lung in CT images using deep learning approaches. The radiologist's difficult work is to determine the malignancy of lung illnesses; thus, deep learning models aid much in this effort since lung cancer pictures show varying degrees of opacity in the region of interest. This is a texture-based challenge in which 42 CT pictures with high and low malignant degrees of malignancy are gathered. Machine learning algorithms are being used to categorise lung pictures [12]. Deep learning algorithms can improve classification accuracy, allowing for the categorization of malignant and non-cancerous images. Different classifiers were used in the work [13], including decision trees and support vector machines, as these give greater classification accuracy. The model obtains an accuracy of 94% when using a Convolutional neural network classifier, and an accuracy of 86% when using an SVM classifier. When compared to these classification results, CNN outperforms the SVM classifier. The hybrid segmentation network-based CNN [9] is meant to train CNN models using both 2D and 3D information. This model performs well, with an accuracy of 88%, an average sensitivity of 87.2%, and an average precision of 90.9%. The author suggests Convolutional neural network [15], which reduces the percentage of false positives and improves classification accuracy to 91.23% for diagnosing disorders. Using a deep neural network, the suggested technique improves accuracy to 97% [11], reducing time complexity while increasing accuracy. According to the literature study, numerous writers employed various methodologies for categorization of lung nodules to categorise and diagnose lung cancer in its early stages. According to the review, VGG-16 with deep learning features is one of the most efficient methods for classifying malignant photos. When a VGG-16 is used for deep learning classification features, it is referred to as the Improved VGG-16, and it performs a bigger number of computations by employing hidden layers, Convolutional layers, SoftMax layer, and fully connected layer. As a result, an Improved VGG-16 performs the classification operation efficiently and precisely.

III. ARCHITECTURE IN PROPOSITION

The VGG model, which stands for the Visual Geometry Group from Oxford, was simpler and deeper than AlexNet. All network layers used 3 by 3 filters with stride and pad size 1 and max pooling size 2 with stride 2. Although the size decreases due to max pooling, the number of filters increases with layers. The architecture utilised for the image classification model is VGG-16, as shown in Figures 2 and 3, although the architecture has 16 layers, as stated in Table 1. The architecture in the table illustrates each layer depth, kernel size of pooling filters, strides, Rectified Linear Unit (ReLU) is the most often used activation function in image classification, and a SoftMax activation loss function was employed at the end classification task. Figure 1 depicts a simple CNN architecture with hidden and thick layers for feature extraction and classification.

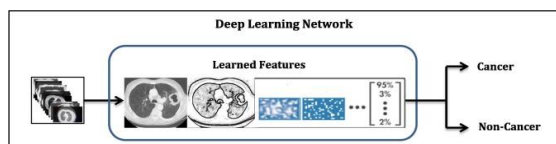


Fig:1 Elementary CNN Architecture

The following layers comprise the fundamental CNN architecture.

1. Convolution Layer: These layers have kernels, Stride and Padding.
2. Pooling Layer: It decreases the parameters needed in computing by reducing the dimension of the picture.
3. Fully Connected Layer: This layer assigns a label to the photos from the previous two levels. Because this layer uses the SoftMax layer to determine the probabilities between 0 and 1.

A. THE VGG-16 NETWORK MODEL

The VGG model, which stands for the Visual Geometry Group from Oxford, is simpler and more in-depth than AlexNet. All network layers used 3X3 filters with stride and pad sizes of 1 and a maximum pooling size of 2. Figure 2 depicts the VGG-16 architectural block diagram, which comprises of sixteen layers, thirteen convolution layers, five max-pooling layers, and three fully-connected layers with SoftMax layer. Finally, a completely linked layer incorporating the SoftMax layer determines whether or not the lung cancer is contained.

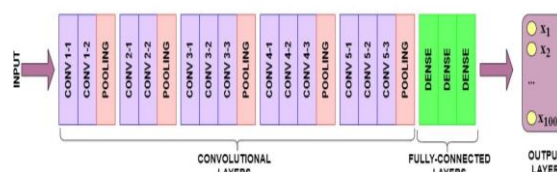


Fig:2 Structure of the VGG-16 Model

| Layer | Depth | Filter/Pooling | Stride |
|-----------------------|-------|----------------|--------|
| | | VGG-16 | |
| Input | 3 | - | - |
| Convolution1 | 64 | 3 X 3 | 1 X 1 |
| ReLU | - | - | - |
| Convolution2 | 64 | 3 X 3 | 1 X 1 |
| ReLU | - | - | - |
| Max-pooling | 64 | 3 X 3 | 2 X 2 |
| Convolution3 | 128 | 3 X 3 | 1 X 1 |
| ReLU | - | - | - |
| Convolution4 | 128 | 3 X 3 | 1 X 1 |
| ReLU | - | - | - |
| Max-pooling | 128 | 3 X 3 | 2 X 2 |
| Convolution5 | 256 | 3 X 3 | 1 X 1 |
| ReLU | - | - | - |
| Convolution6 | 256 | 3 X 3 | 1 X 1 |
| ReLU | - | - | - |
| Convolution6 | 256 | 3 X 3 | 1 X 1 |
| ReLU | - | - | - |
| Max-pooling | 256 | 3 X 3 | 2 X 2 |
| Convolution7 | 512 | 3 X 3 | 1 X 1 |
| ReLU | - | - | - |
| Convolution8 | 512 | 3 X 3 | 1 X 1 |
| ReLU | - | - | - |
| Convolution8 | 512 | 3 X 3 | 1 X 1 |
| ReLU | - | - | - |
| Max-pooling | 512 | 3 X 3 | 2 X 2 |
| Convolution8 | 512 | 3 X 3 | 1 X 1 |
| ReLU | - | - | - |
| Convolution8 | 512 | 3 X 3 | 1 X 1 |
| ReLU | - | - | - |
| Convolution8 | 512 | 3 X 3 | 1 X 1 |
| ReLU | - | - | - |
| Max-pooling | 512 | 3 X 3 | 2 X 2 |
| Fully connected Layer | 4096 | - | - |
| Fully connected Layer | 4096 | - | - |
| Fully connected Layer | 1000 | - | - |
| Output | 2 | - | - |

Table:1 VGG-16 Architecture Specifications

B. A BETTER VGG-16 MODEL

Improved VGG-16 is a modified version of VGG-16 that was created to improve accuracy. The network's depth, kernel size, and extracted feature maps are employed for the building of the Improved VGG-16 network model illustrated in Figure 3, which detects malignant or benign at the output.

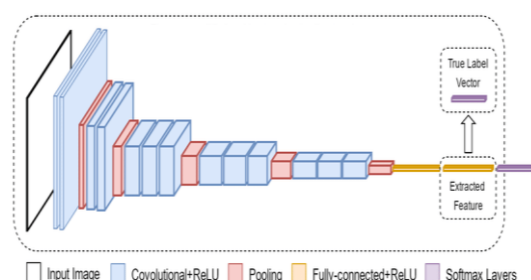


Fig:3 VGG-16 Model Architecture Improvements

| Algorithm of Bettered VGG-16 Model | |
|------------------------------------|---|
| ▪ | Using an existing LIDC dataset and an augmentation approach, get pictures of Lung Cancer that include both diseased and non-diseased cells. |
| ▪ | Preprocess all photos to 224X224X3 using the VGG-16 technique. Assign benign and malignant class labels to the photos. |
| ▪ | Categorize the photos in the training and testing datasets using all of the class labels. |
| ▪ | Train the Improved VGG-16 Model using 80% of the training pictures. Using 20% testing photos, put the Improved VGG-16 Model to the test. Determine the different performance measurement metrics. |
| ▪ | Validate the suggested Model's performance. |

Algorithm:1 Bettered VGG-16 Model Algorithm

A bettered VGG-16 architecture block diagram is illustrated in Algorithm 1 and comprises of 18 layers, which include fifteen convolution layers, fifteen Rectified Linear Unit levels, six max-pooling layers, and three fully-connected layers with SoftMax layer. The input picture of size 224x224x3 is applied to the network's first convolution layer, but the network model ultimately chooses whether or not the image contains lung cancer.

| Layer | Depth | Filter/Pooling | Stride |
|-----------------------|-------|----------------|--------|
| | | VGG-16 | |
| Input | 3 | - | - |
| Convolution1 | 64 | 3 X 3 | 1 X 1 |
| ReLU | - | - | - |
| Convolution2 | 64 | 3 X 3 | 1 X 1 |
| ReLU | - | - | - |
| Max-pooling | 64 | 3 X 3 | 2 X 2 |
| Convolution3 | 128 | 3 X 3 | 1 X 1 |
| ReLU | - | - | - |
| Convolution4 | 128 | 3 X 3 | 1 X 1 |
| ReLU | - | - | - |
| Max-pooling | 128 | 3 X 3 | 2 X 2 |
| Convolution5 | 256 | 3 X 3 | 1 X 1 |
| ReLU | - | - | - |
| Convolution6 | 256 | 3 X 3 | 1 X 1 |
| ReLU | - | - | - |
| Convolution6 | 256 | 3 X 3 | 1 X 1 |
| ReLU | - | - | - |
| Max-pooling | 256 | 3 X 3 | 2 X 2 |
| Convolution7 | 512 | 3 X 3 | 1 X 1 |
| ReLU | - | - | - |
| Convolution8 | 512 | 3 X 3 | 1 X 1 |
| ReLU | - | - | - |
| Convolution8 | 512 | 3 X 3 | 1 X 1 |
| ReLU | - | - | - |
| Max-pooling | 512 | 3 X 3 | 2 X 2 |
| Convolution8 | 512 | 3 X 3 | 1 X 1 |
| ReLU | - | - | - |
| Convolution8 | 512 | 3 X 3 | 1 X 1 |
| ReLU | - | - | - |
| Max-pooling | 512 | 3 X 3 | 2 X 2 |
| Convolution9 | 512 | 3 X 3 | 1 X 1 |
| ReLU | - | - | - |
| Convolution10 | 512 | 3 X 3 | 1 X 1 |
| ReLU | - | - | - |
| Max-pooling | 512 | 3 X 3 | 2 X 2 |
| Fully connected Layer | 4096 | - | - |
| Fully connected Layer | 4096 | - | - |

| | | | |
|-----------------------|------|---|---|
| Fully connected Layer | 1000 | | - |
| Output | 2 | - | - |

Table 2 Specifications of the Better VGG-16 Architecture

C. BETTER VGG-16 MODEL TRAINING

In both VGG-16 Models, 80% of CT scans were utilised for training and 20% for testing, resulting in classification accuracy, which controls the degree of properly categorising the pictures as benign or cancerous.

D. CONFUSION MATRIX

| | | True Class | |
|-----------------|----------|------------|----------|
| | | Positive | Negative |
| Predicted Class | Positive | TP | FP |
| | Negative | FN | TN |

Fig:4 Confusion Matrix

Confusion Matrix: Confusion Matrix determines the amount of prediction of a classification model by correlating label and model categorization. It is a two-by-two table composed of four binary classifier results marked as TP, FP, TN, and FN. Where TP denotes true positives, FP denotes false positives, TN denotes true negatives, and FN denotes false negatives. The performance measure parameters are shown in Table 3.

Parameters for Measuring Performance

Medical image performance may be evaluated using performance assessment metrics.

- **Accuracy:** The most common metric used to evaluate the model is accuracy. It is calculated as a proportion of the total number of properly categorised pixels to the total number of pixels in the picture.
- **Loss Function:** Loss is a critical component of Neural Networks. Loss is nothing more than a Neural Net prediction mistake. And the procedure for calculating the loss is known as the Loss Function.
- **Computation Time:** It is the amount of time needed for the process to finish its computation or activities. When a process is simple, it takes less time to process than a complicated process, which requires more computing time.
- **Error rate:** The error rate (ERR) is derived by dividing the total number of inaccurate predictions by the total number of observations in the dataset. The best error rate is zero, while the worst is one.
- **The F1-score** represents a harmonic mean of accuracy and recall.
- **Sensitivity (Recall):** The number of correct positive predictions divided by the total number of positives is referred to as sensitivity (SN). It accurately predicts the positive class and is also known as the true positive rate (TPR).
- **Specificity:** Specificity (SP) is calculated by dividing the number of valid negative predictions by the total number of negatives. It accurately predicts the negative class and is also known as the real negative rate (TNR).
- **Precision:** Precision (PREC) is defined as the number of correct positive predictions divided by the total number of positive predictions. It is often referred to as positive predictive value (PPV).
- **False positive rate (FPR):** The false positive rate (FPR) is defined as the number of wrong positive predictions divided by the total number of negatives, and it forecasts the positive class incorrectly.
- **False negative rate (FNR):** It forecasts the negative class wrongly and the reverse of the false positive rate.
- **False discovery rate (FDR):** It is a way of thinking about the rate of Type-I mistakes in null hypothesis testing while performing multiple comparisons.

- Prevalence: It is the proportion of the positive sum to the overall population.
- Positive likelihood Ratio (PLR): $PLR = \frac{Sensitivity}{(1-Specificity)}$

Table:3 Criteria for Performance Evaluation

IV. RESULTS AND DISCUSSIONS

Deep learning performs well in picture categorization, as demonstrated by models such as AlexNet and VGGNet. VGG-16 is deeper than AlexNet because it has greater feature learning ability [11]. The LIDC dataset collection is a global imaging resource for assessing and diagnosing lung

cancer. It comprises of 1018 CT scans in DICOM format. The original photos are 512×512 in size, however it is difficult to train huge images in the VGG16 network model, thus pre-processed images with reduced dimension suited for the network were used. As a result, training and testing photos are categorised in order to evaluate the network for effective categorization of images into malignant and non-cancerous images, which aids in early diagnosis of the patient [4][5].

A. RESULT OF THE VGG-16 MODEL

According to Fig. 7, when epochs grow towards the higher end, the Accuracy curve climbs towards the higher end, and hence accuracy increases.

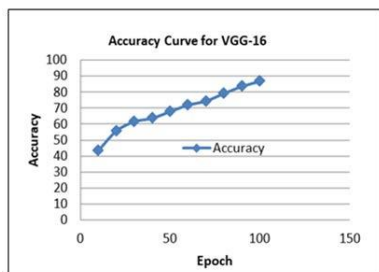


Fig:6 VGG-16 Accuracy Curve

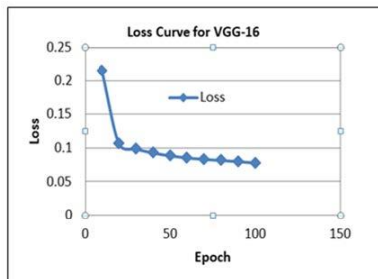


Fig:7 VGG-16 Loss Curve

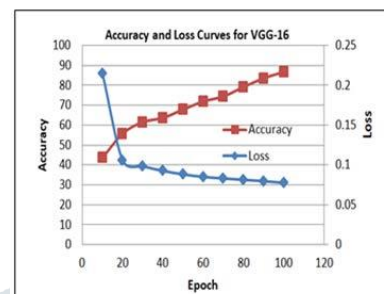


Fig:8 VGG-16 Accuracy and Loss Curves

- According to Fig. 7, when epochs go towards the higher end, the loss curve drops and hence the loss diminishes.

- Fig:8 depicts the accuracy and loss curves, as well as their relationship with respect to epoch.

| VGG-16 Performance Measure Parameter (a) | | | | | | | | | | |
|--|--------|------------------------|----------|------------|--------|--------|--------|--------|--------|--------|
| Parameters | Loss | Computation Time (sec) | F1 Score | Error Rate | TPR | FPR | TNR | FNR | BA | PPV |
| VGG-16 | 0.0383 | 410 | 0.9610 | 0.0300 | 0.9608 | 0.0392 | 0.9796 | 0.0204 | 0.9808 | 0.9608 |

Table:4a VGG-16 Parameters for Measuring Performance

| VGG-16 Performance Measure Parameters (b) | | | | | | |
|---|------|------------|------|-------|---------|--------|
| Parameters | FDR | Prevalence | PLR | NLR | DOR | TS |
| VGG-16 | 0.12 | 0.52 | 7.33 | 0.190 | 38.5963 | 0.7462 |

Table:4b VGG-16 Parameters for Measuring Performance

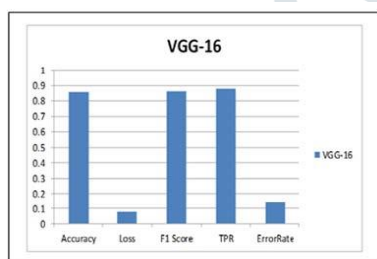


Fig:10a VGG-16 Performance Measure Parameters

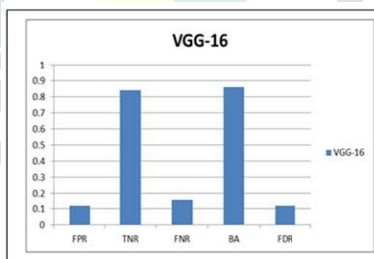


Fig:10b VGG-16 Performance Measure Parameters

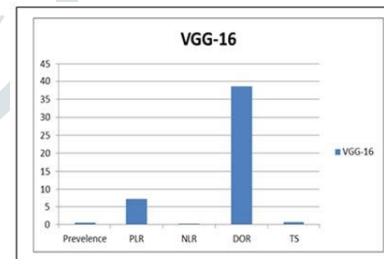


Fig:10c VGG-16 Performance Measure Parameters

B. BETTER VGG-16 MODEL RESULTS

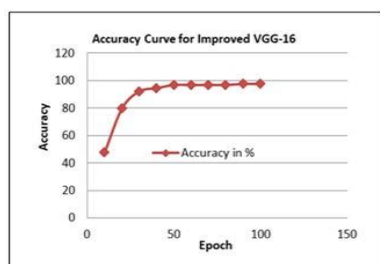


Fig:11 The Better VGG-16's accuracy curve

- According to Fig. 11, when epochs grow towards the higher end, the Accuracy curve climbs towards the higher end, and hence accuracy increases.
- According to Fig. 12, when epochs grow towards the higher end, the loss curve reduces towards the higher end, and therefore the loss diminishes.

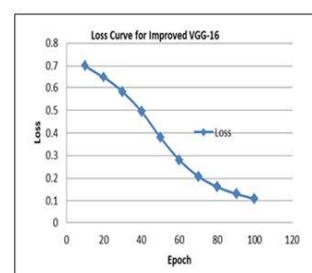


Fig:12 Bettered VGG-16 Loss Curve

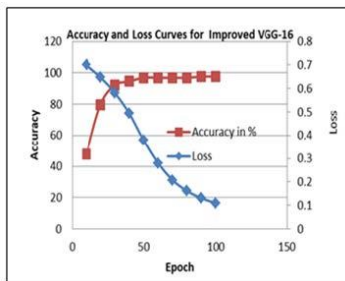


Fig:13 For the enhanced VGG-16, accuracy and loss curves

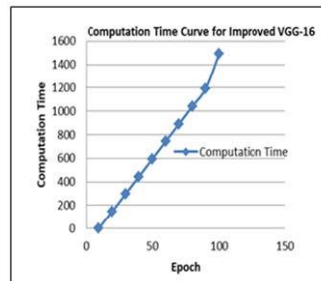


Fig:14 Time to Compute for the Improved VGG-16

- Fig. 14 indicates that when the period near the upper end, computation time increases because more computation requires more computation time and therefore computation time increases.

| Bettered VGG-16 Performance Measure Parameters | | | | | | | | | | |
|--|----------|--------|------------------------|----------|------------|--------|-------|-----|--------|------|
| Parameters | Accuracy | Loss | Computation Time (sec) | F1 Score | Error Rate | TPR | FPR | TNR | FNR | BA |
| Improved VGG-16 | 0.9700 | 0.1092 | 1490 | 0.9708 | 0.0300 | 0.9433 | 0.055 | 1 | 0.0002 | 0.97 |

Table:5a Bettered VGG-16 Performance Measure Parameters

| Parameters for Performance Measurement of the bettered VGG-16 | | | | | | |
|---|--------|------------|-------|--------|-----|-------|
| Parameters | FDR | Prevalence | PLR | NLR | DOR | TS |
| Improved VGG-16 | 0.0566 | 0.5 | 16.63 | 0.0002 | 0 | 0.943 |

Table:5b Bettered VGG-16 Performance Measure Parameters

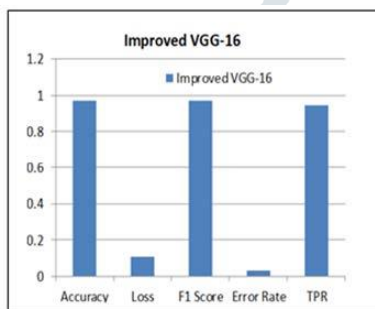


Fig:15a Bettered VGG-16 Performance Measure Parameters

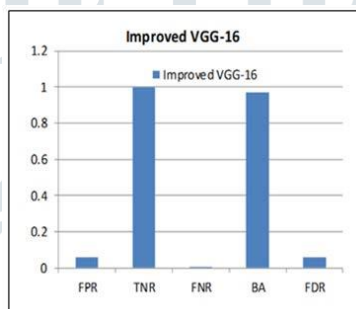


Fig:15b Bettered VGG-16 Performance Measure Parameters

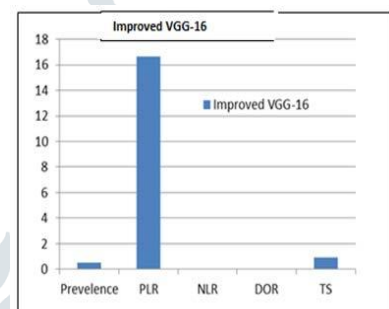


Fig:15c Bettered VGG-16 Performance Measure Parameters

| VGG-16 and Bettered VGG-16 Performance Measure Parameters Comparison | | | | | | | | | | |
|--|----------|--------|-----------------------|----------|------------|-------|--------|------|--------|--------|
| Parameters | Accuracy | Loss | Computation Time(sec) | F1 Score | Error Rate | TPR | FPR | TNR | FNR | BA |
| VGG-16 | 0.86 | 0.0776 | 554 | 0.8627 | 0.14 | 0.88 | 0.12 | 0.84 | 0.16 | 0.86 |
| Improved VGG-16 | 0.97 | 0.1092 | 1490 | 0.9708 | 0.03 | 0.943 | 0.0567 | 1 | 0.0002 | 0.9717 |

Table:6a Performance Comparison

| VGG-16 and Bettered VGG-16 Performance Measure Parameters Comparison | | | | | | |
|--|-------|------------|--------|--------|-------|--------|
| Parameters | FDR | Prevalence | PLR | NLR | DOR | TS |
| VGG-16 | 0.12 | 0.52 | 7.33 | 0.79 | 38.59 | 0.7462 |
| Improved VGG-16 | 0.056 | 0.5 | 16.636 | 0.0002 | 0 | 0.943 |

Table:6b Performance Comparison

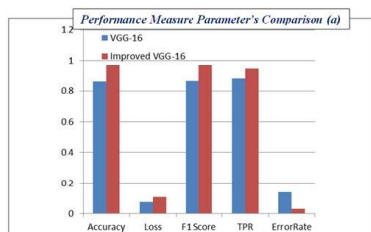


Fig:16a Comparison of Performance Metrics

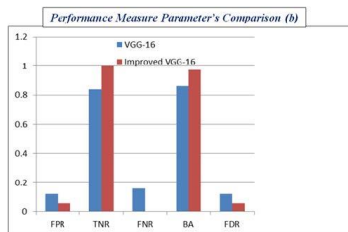


Fig:16b Comparison of Performance Metrics

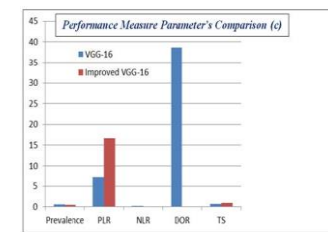


Fig:16c Comparison of Performance Metric

The proposed lung cancer classification and identification models were created in MATLAB 2018b, and the results show that classification accuracy increases as training progresses and loss percentage decreases, but for the entire process, the VGG-16 model provides an accuracy of 86% and precision of 88% in 554 seconds, while the Improved VGG-16 model provides an accuracy of 97% and precision of 94.34% in 1490 seconds. The dataset utilised for training and testing purposes in this study was acquired from LIDC-IDRI and was used to feed the network model, which is capable

of detecting and identifying malignant (Malignant Images) and non-cancerous malignancies (Benign Images). According to the results, as training progresses, classification accuracy rises with increasing computation time, lowering the percentage of loss as indicated in the output graphs above. The whole procedure of the Improved VGG-16 models yields 97% accuracy with a calculation time of 1490 seconds in GPU workstation, which is the highest degree of accuracy produced when compared to previous research articles [12].

V. CONCLUSION

In this article, an improved version of VGG-16 convolutional neural networks was constructed for categorising CT images of lung cancer tumours as benign or malignant. Thus, prior to applying the input CT images to the network model, pre-processing was performed to ensure that the pictures

were of comparable size and format. The dataset utilised in this study comes from the LIDC dataset, hence the accuracy of an Improved VGG-16 model developed is 97%, which is equivalent to the 86% accuracy of VGG-16. Thus, VGG-16 has an accuracy of 86%, but Improved VGG-16 has an accuracy of 97%, indicating that Improved VGG-16 outperforms VGG-16 in lung tumour picture detection and classification.

VI. COMPLIANCE WITH ETHICAL STANDARDS

Funding: This study was funded by none.

Conflict of Interest: None.

Ethical approval: This article does not contain any studies with human participants or animals performed by any of the author.

REFERENCES

- [1] Jiang, H., Qian, , Gao, M., Li, Y. "An automatic detection system of lung nodule based on multigroup patch-based deep learning network" IEEE Journal of Biomedical and Health Informatics, 22(4), pp.1227-1237, 2012
- [2] Disha Sharma, Gagandeep Jindal, "Identifying Lung Cancer Using Image Processing Techniques", International Conference on Computational Techniques and Artificial Intelligence, pp. 116-120, 2011.
- [3] Farzad Vasheghani Farahani "Lung Nodule diagnosis from CT images Based on Ensemble Learning." IEEE Conference on Computational Intelligence in Bioinformatics and Computational Biology, 2015.
- [4] Xin-Yu Jin, Yu-Chen Zhang, Qi-Liang Jin "Pulmonary Nodule Detection Based on CT Images Using Convolution Neural Network." 9Th International Symposium on Computational Intelligence and Design. 2016.
- [5] Ryota Shimizu, Shusuke Yanagawa, Yasutaka Monde, Hiroki Yamagishi, Mototsugu Hamada, Toru Shimizu, and Tadahiro Kuroda "Deep Learning Application Trial to Lung Cancer Diagnosis for Medical Sensor Systems" International Symposium on Computers and Communications, 2016.
- [6] Po-Whei Huang, Phen-Lan Lin, Cheng-Hsiung Lee, C. H. Kuo, "A Classification System of Lung Nodules in CT Images Based on Fractional Brownian Motion Model", IEEE International Conference on System Science and Engineering, July 2016.
- [7] Vaishali C. Patil, Shrinivas R. Dhotre, "Lung Cancer Detection from Images of Computer Tomography Scan", International Journal of Advanced Research in Computer and Communication Engineering, Vol. 5, Issue 7, July 2016.
- [8] Ailton Felix, Marcelo Oliveira, Aydano Machado, Jose Raniery, "Using 3D Texture and Margin Sharpness Features on Classification of Small Pulmonary Nodules" ,29th SIBGRAPI Conference on Graphics, Patterns and Images, 2016.
- [9] Sri Widodo, Ratnasari Nur Rohmah, Bana Handaga, "Classification of Lung Nodules and Arteries in Computed Tomography Scan Image Using Principal Component Analysis" 2nd International Conferences on Information Technology, Information Systems and Electrical Engineering, 2017.
- [10] Rabindranath K , K Soma Shekar, "Early Detection of lung cancer by nodule extraction – A Survey", International Conference on Electrical, Electronics, Communication, Computer and Optimization Techniques , 2017.
- [11] Rui Xu, Jiao Pan, Xinchun Ye, Yasushi Hirano, Shoji Kido, Satoshi Tanaka "A Pilot Study to Utilize a Deep Convolutional Network to Segment Lungs with Complex Opacities" Chinese Automation Congress, 2017.
- [12] Anna Poreva, Yevgeniy Karplyuk, Valentyn Vaityshyn, "Machine Learning Techniques Application for Lung Diseases Diagnosis", 5th IEEE Workshop on Advances in Information, Electronic and Electrical Engineering, 2017.
- [13] LIDC-IDRI, <https://wiki.cancerimagingarchive.net/display/Public/LIDC-IDRI>.